ace-21334.pdf

by

Submission date: 30-Nov-2022 10:12AM (UTC+0700)
Submission ID: 1966850001
File name: ace-21334.pdf (2.22M)
Word count: 2451
Character count: 13286

Modeling Reinforced Concrete Beam with GFRP Bar and GFRP Sheet Using Finite Element Method.

E A Z Ikhsan[1], H Parung[2], and R Irmawaty[3]

[1]Master student, Department of Civil Engineering, Universitas Hasanuddin, Indonesia
[2]Professor, Department of Civil Engineering, Universitas Hasanuddin, Indonesia
[3]Associate Professor, Department of Civil Engineering, Universitas Hasanuddin, Indonesia

erikaikhsan@yahoo.com

Abstract. The use of FRP bar reinforcement as a rust-resistant material is one solution to increase the resilience of reinforced concrete structures in the marine environment. Innovations in the use of FRP reinforcement need to be developed to improve quality and reduce construction costs by eliminating concrete cover and shear reinforcement. Removing the concrete cover and shear reinforcement in the beam can minimize the cross-sectional height without reducing the effective height of the beam and simplify the placing of concrete. To replace the shear reinforcement, GFRP sheets are installed in the shear span. To validate the flexural behavior of reinforced concrete beams using FRP rods without concrete cover with GFRP sheet shear reinforcement in the experimental study, a numerical analysis was carried out using the finite element method using abaqus cae software. modeling and treatment of test objects in numerical analysis is based on modeling and experimental treatment studies including material data used are the same as those in experimental research. The results obtained are that the flexural load capacity of the BFTS analyzed numerically is 12.45% greater than the experimental study. BFTS crack pattern in numerical analysis is wider than experimental study because the load resisted is numerically larger but basically the crack pattern experienced in the mid-span zone is similar.

Keywords: Numerical analysis, Experimental study, GFRP sheet and GFRP bar

1. Introduction

The use of corrosion-resistant reinforcement on structural elements for very aggressive environmental conditions is more profitable than the use of steel reinforcement that is given rust protection by catodic protection, epoxy coating or galvanization methods [1]. In addition to being corrosion resistant, GFRP bars have high strength, are not affected by magnetism, have good fatigue resistance, are lightweight, have low thermal and electrical conductivity [2].

Meanwhile, repairs due to shear reinforcement damage can be done by adding GFRP sheet as needed. Glass fiber materials have a more elastic strain energy capacity and a high strength to weight ratio compared to steel, as a result, the use of steel in concrete will be reduced. GFRP bars are more suitable for designing structural elements, demanding a high strength-to-weight ratio as well as high corrosion resistance.

The results of previous studies showed that beams with GFRP reinforcement were able to increase the flexural capacity of beams by 4.14% against normal beams [3]. Meanwhile, other experimental results show that the installation of GFRP sheet on the beam can increase the flexural capacity and

ductility of the beam. They are 37.96% and 25%, respectively [4].

This paper aims to validate the experiment research with a finite element program. This paper is comperation and validation of experimental study of Kusnadi in 2020. Are the results of the numerical analysis in accordance with the results of the experimental study, it is necessary to conduct a study entitled "Modeling Reinforced Concrete Beams with Glass Fiber Reinforced Polymer (GFRP) Bars and Sheets Using Finite Element Method". Also, this analysis is expected as a reference material in the planning and repair of structures, especially in structures in the marine environment by considering the advantages and disadvantages of using GFRP bars and GFRP sheets.

2. Materials

2.1. Material properties

The materials used in are concrete fc' 25 MPa, steel Ø8, steel D13, GFRP bar D13 and GFRP sheet 1,3 mm.

(a) Concrete (b) Steel (c) GFRP bar (d) GFRP sheet

Figure1. The materials used

2.1.1. Concrete damage plasticity (CDP)

In this analytical study, CDP was chosen because compared to other models, CDP is able to simulate the elastic and plastic properties of concrete by considering the softening behavior in both compression and tension. CDP relies on two main failure patterns to control the behavior of concrete elements; compression crushing and tensile cracking. There are five standard parameters that Abaqus provides to solve functions.

Table 1. Concrete behavior.

Material	Compression Strength fc' (MPa)	Tensile Strength fct (MPa) Kusnadi. 2021	Elastic Modulus (MPa) Hamid Sinaei dkk. 2012	Poisson's Ratio (MPa)	Density (tonne/mm3)
Concrete	25	0,50√fc' = 2,5	4700√fc' = 23500	0,21	$2{,}4 \times 10^{-9}$

Table 2. Parameter plasticity untuk concrete damage plasticity

Dilation angle	Eccentricity	$\frac{f_{b0}}{f_{c0}}$	K	Viscosity parameter
20	0.1	1.16	0.667	0

(Source: Walid Mansour, 2021)

The tensile damage parameter, dt is defined as the ratio of the cracking strain to the total strain. Similarly, the compressive damage parameter, dc is defined as the ratio between the inelastic strain and total strain. If damage parameters are not specified, the model behaves as a plasticity model.

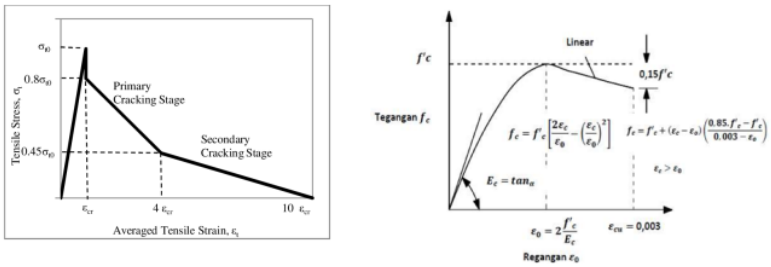

(a) in tension [5] (b) in compression [6].

Figure 2. behavior of concrete

2.1.2. Steel

Steel is an isotropic material, the input data on abaqus uses density, plasticity and elastic data. Plastic behavior filled with yield stress and plastic stain values. Young's modulus value and poisson's ratio for the elastic and mass density for density.

2.1.3. GFRP (Glass Fiber Reinforced Polymer) bar

Modulus of elasticity of GFRP bars (40-55 GPa) is lower than that of steel bars leading to larger deflections and wider cracks than steel-reinforced concrete, this is why GFRP bars are not usually used as compression reinforcement [7]. GFRP bar is an anisotropic material with a strong longitudinal axis governed by fibers and a weak or moderate transverse axis regulated by a fiber binding resin [8].

GFRP bar material is an isotropic material, the data input on abaqus uses density, plasticity and elastic data. Elastic behaviors are young's modulus and the position ratio, and mass density for density behavior.

Table 3. Reinfrocements behavior

Material	Ultimate Stress (MPa)	Elastic Modulus (MPa)	Poisson's Ratio (MPa)	Density (tonne/mm3)
GFRP bar (D13 mm)	788	43900	0,25	2,1 x 10-9
GFRP Sheet (1.3 mm)	575	26100	0,33	2,6 x 10-9
Steel (D13 mm)	370	200000	0,3	7,85 x 10-9
Steel (ø8 mm)	240	200000	0,3	7,85 x 10-9

2.1.4. Hashin damage GFRP (Glass Fiber Reinforced Polymer) sheet

GFRP Sheet is an orthotropic elastic material [9] and based on the (Abaqus Analysis User's Guide) the behavior of the glass fiber reinforced epoxy coating material is assumed to be orthotropic, with a stiffer response along the fiber direction and a more pronounced behavior soft in the matrix. Where the material data uses density, elastic type lamina and hashin damage.

Material behavior elastic for GFRP sheet using lamina type. Although based on abaqus manual version 6.14, GFRP sheet is assumed to be orthotropic, but the mechanical properties of advanced composite laminates are assumed for better mathematical modeling in structural analysis. Where the lamina itself in the big Indonesian dictionary means a thin sheet. Each lamina was treated as an orthotropic material under a field stress state and assumed to be transverse isotropic [10]. GFRP Sheet using Hashin damage, [11] proposed that the criteria for predicting the failure of composite materials should be based on the mechanism of material failure.

Hashin [11] proposed that the criteria for predicting the failure of composite materials should be based on the failure mechanism of the material, not simply extrapolating existing criteria to other materials as was the case in the Tsai-Hill and Tsai-Wu Criteria. These failure criteria are used to predict

different failure modes such as fiber breakage in stress, fiber buckling in compression, matrix cracking, and debonding. The spesimen uses the Hashin-Rotem criteria, 1973 because the material is in a state of biaxial stress, the alpha value in the material behavior is equal to 0.

Table 4. Initial orthotropic damage properties of fiber-reinforced epoxy.

Longitudinal Failure Stresses		Transverse Failure Stresses		Longitudinal & Transversal
Tensile	Compression	Tensile	Compression	in-Plane Shear Strength
$\sigma_L^{f,t}$ (Mpa)	$\sigma_L^{f,c}$ (Mpa)	$\sigma_T^{f,t}$ (Mpa)	$\sigma_T^{f,c}$ (Mpa)	τ_{LT}^{f} (Mpa)
2500	2000	50	150	50

Source: Abaqus user manual 6.14

2.2. Modeling specimens

The specimen is BFTS, fiber beam without cover concrete. Where dimention of the beam 150x250x3300 mm. The specimen uses some materials. It uses concrete fc' 25 MPa, steel Ø8 as compressive reinforcement, GFRP bar D13 as tensile reinforcement, and GFRP sheet as shear reinforcement. Figure 3 shows the beam using GFRP bars as tensile reinforcement and GFRP sheets as shear reinforcement without covers (BFTS).

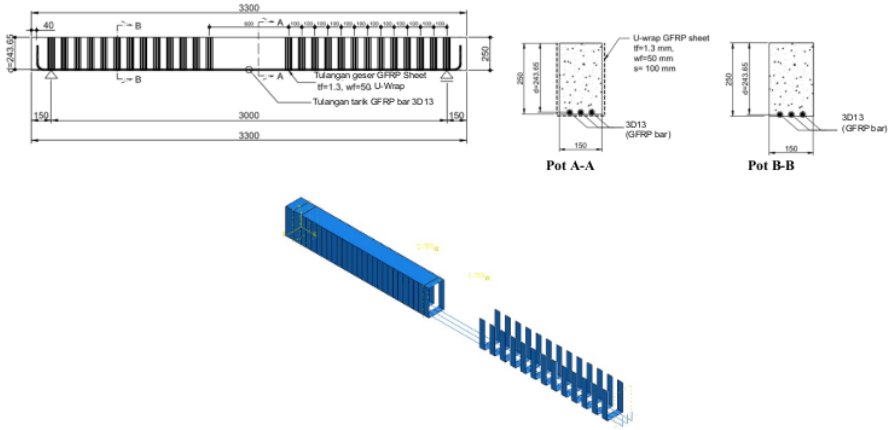

Figure 3. Modeling scheme of fiber beam without cover concrete (BFTS).

2.3. Modelling of the interface surface between concrete and gfrp sheet

The model is simulated using a perfect bond as a tie constraint where no separation between the two surfaces is allowed [12]. The value of friction is obtained from the product of the coefficient of friction and the nominal stress. Table 5 shows the coefficient of friction for the unsmoothed concrete surface is 0.60 while equation (1) shows that the nominal stress value reaches one [12]

$$\{\frac{\sigma_n}{\sigma_{nmax}}\}^2 + \{\frac{\tau_t}{\tau_{tmax}}\}^2 + \{\frac{\tau_s}{\tau_{smax}}\}^2 = 1.0 \quad (1)$$

Where σ_n is the tensile stress of the interface in MPa units, τ_t and τ_s are the interfacial shear stress, n tandsubscripts represent the direction of the adhesive thickness of the stress component in mm, σ_{nmax} is the maximum tensile strength of the cohesive surface. While σ_{t0}, τ_{tmax} and τ_{smax} are the maximum shear strength of the cohesive surface.

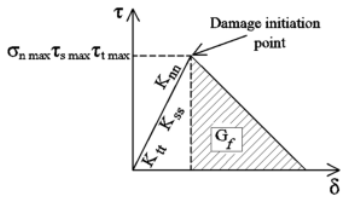

Figure 4. Traction separation modeling (tensile) for a cohesive surface.
Source: walid manosur, 2021

Table 5. Cohesion and friction coefficient values

Surface characteristics of the interface	c	μ	Ra (mm)
Very smooth (steel, plastic, specially treated timber formwork)	0,025	0,50	Not measurable
Smooth (concrete surface without curing)	0,35	0,60	< 1,5
Rough (strongly roughened surface)	0,45	0,70	≥ 1,5
Very rough	0,50	0,90	≥ 3,0

Source : fib Model-Code (2010)

friction = μ σ_n = 0,60 x 1 = 0,60
Therefore for the coefficient of shear between the surfaces is 0.60.

3. Result and discussions

3.1. Load-deflection curve

Figure 5 shows the load and deflection responses of numerical analysis result and kusnadi's experimental study which are summarized in Table 5. The deflection reported here was the deflection at the mid-span of the beam. Generally, all the beams exhibited similar behavior until the first crack. After that, the slope of load-deflection curves reduced differently. The curve of mesh 50 is higher than mesh 40, then curve of mesh 40 is higher than mesh 30. Meanwhile, the stiffness of mesh 30 and mesh 40 is almost similar. This indicates that the use of mesh value at abaqus cae affected the stiffness of the beams. The shape of numerical analysis curve is different to kusnadi's experimental study curve in 2021.

As shown in Table 6, average maximum load value of numerical analysis is 78.83 kN which is higher than the experimental study 75.08 kN. This shows that there are factors in the experimental study that cause the results of the beam in the experimental study to be less able to resist 3.75kN, with a higher accepted load, the beam analyzed numerically also only experienced 42% smaller deflection of the experimental study deflection experienced. The load was constant, while the displacement still increased until the failure. This was a typical flexural failure mode.

Table 6. Results of numerical and experiment analysis

Specimens	Load (Pu) (kN)	Deflection (Δu) (mm)
BFTS-mesh 30	69,076	32,564
BFTS-mesh 40	75,339	41,431
BFTS-mesh 50	92,07	42,423
Average Numerical	**78,828**	**38,806**
Average Experiment	**75,08**	**68,91**

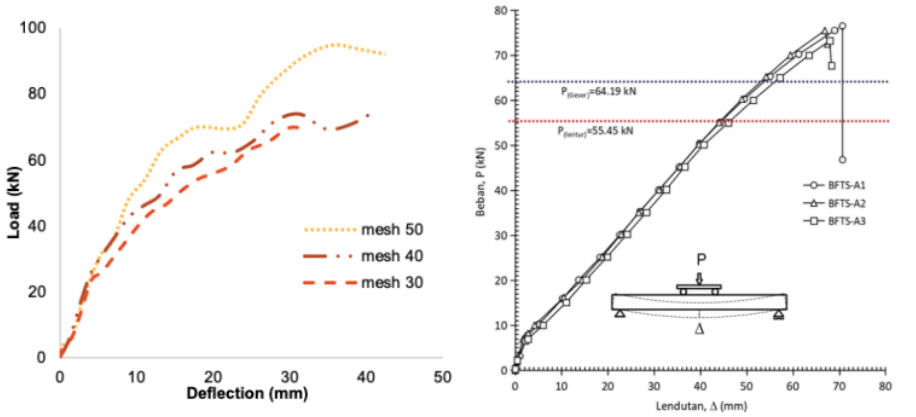

(a) Numerical analysis (b) Kusnadi's Experimental study in 2020

Figure 5. Load-deflection responses of BFTS

3.2. Crack Pattern

Figure 6 and 7 showed the crack pattern of analysis numerical beams and experimental study at the ultimate load. The ultimate load of BFTS mesh 30, mesh 40, mesh 50 and BFTS experimental study were 69.08 kN, 75.34 kN, 92.07 kN, and 75.08 kN, respectively. Comparing to cracks pattern of the experimental study, the pattern of cracks on numerical analysis are wider but still similar. The long cracks were concentrated in the constant moment region at the span center. The mesh 50 pattern indicates that the GFRP sheet performs well to resist cracking under the beam however cracks still occur at the mid span. This was because the concrete of experimental study has not reach maximum load failure as numerical analysis beam can resists.

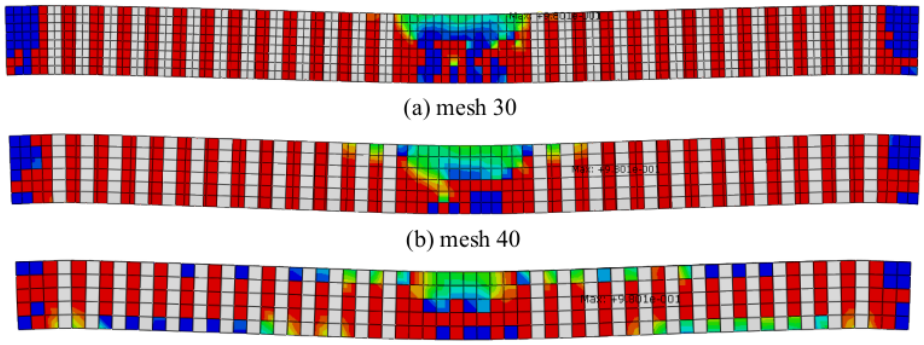

(a) mesh 30

(b) mesh 40

(c) mesh 50

Figure 6. Crack Pattern BFTS at failure of numerical analysis

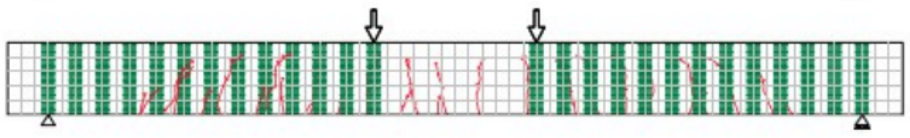

Figure 7. Crack Pattern BFTS at failure of kusnadi's experimental study in 2020

4. Conclusion

The comparation result of fiber beam without cover concrete between analysing with finte element method and experimentak study show that:

1. The flexural load capacity of the BFTS analyzed numerically is 12.45% greater than the experimental study. Although the material data used are the same as those in the experimental study.
2. The BFTS crack pattern in the numerical analysis is wider than the experimental study because the numerically resisted load is greater but basically the crack pattern experienced in the midspan zone is the same.

References

[1] Sultan, Mufti & Djamaluddin, Rudy. (2020). Daktalitas dan Kapasitas Lentur Balok Beton Bertulang dengan Perkuatan GFRP-S. Konferensi Nasional Teknik Sipil 12. Batam, Indonesia.

[2] ACI. Committee 440.2R-08, 2008, Guide for the Design and Construction of Externally Bonded FRP Systems for Strengthening Concrete Structures, American Concrete Institute, U.S.A.

[3] Hijriah, Parung Herman, Djamaluddin Rudy & Irmawaty Rita. (2020). Delaminasi Lembar GFRP pada Balok Beton Bertulang. 18. 1271-1276.

[4] Kusnadi, 2020. Flexural Behavior of GFRP Bar Reinforced Concrete Beam without Concerete Cover at the Tension Zone with GFRP Sheet as Shear Reinforcement. Dissertation for Civil Engineering Department of Hasanuddin University.

[5] Wahalthantri, B., Thambiratnam, D.P., Chan, T.H.T. and Fawzia, S. 2012. An improved method to detect damage using modal strain energy-based damage index. Adv. Struct. Eng., 15, 727-742.

[6] Park, R., & Paulay, T., 1975. Reinforced Concrete Structures. New York, USA: John Wiley & Sons. Inc.

[7] Saraswathy T. & Dhanalakshmi K., 2014. Investigation of Flexural Behaviour of RCC Beams using GFRP Bars. International Journal of Scientific & Engineering Research, Vol 5, Issue 1.

[8] Ahmed, Ehab & El-Salakawy, Ehab & Benmokrane, Brahim. (2010). Performance Evaluation of Glass Fiber-Reinforced Polymer Shear Reinforcement for Concrete Beams. ACI Structural Journal. 107. 53-62.

[9] Alizadeh E, Dehestani M, Navayi Neya B, Nematzadeh M. Efficient composite bridge deck consisting of GFRP, steel, and concrete. Journal of Sandwich Structures & Materials. 2019;21(1):154-174. doi:10.1177/1099636216688347.

[10] Naval Postgraduate School, 2007. Identification of stiffness properties of orthotropic lamina using the experimental natural frequencies and mode shapes. California. pg 5.

[11] Z. Hashin, 1980. Failure criteria for unidirectional fiber composites. Journal of Applied Mechanics, 47, 329-334.

[12] Mansour W., 2021. Numerical analysis of the shear behavior of FRP-strengthened continuous RC beams having web openings. Engineering Structures, Volume 227.

[13] Hognestad, E. 1951. A Study of Combined Bending and Axial Load in Reinforced Concrete Members. Bulletin Series No. 399. University of Illinois Engineering Experiment Station, Urbana, Ill. p.128.

[14] Simulia Abaqus 6.14 user guidance http://130.149.89.49:2080/v6.14/

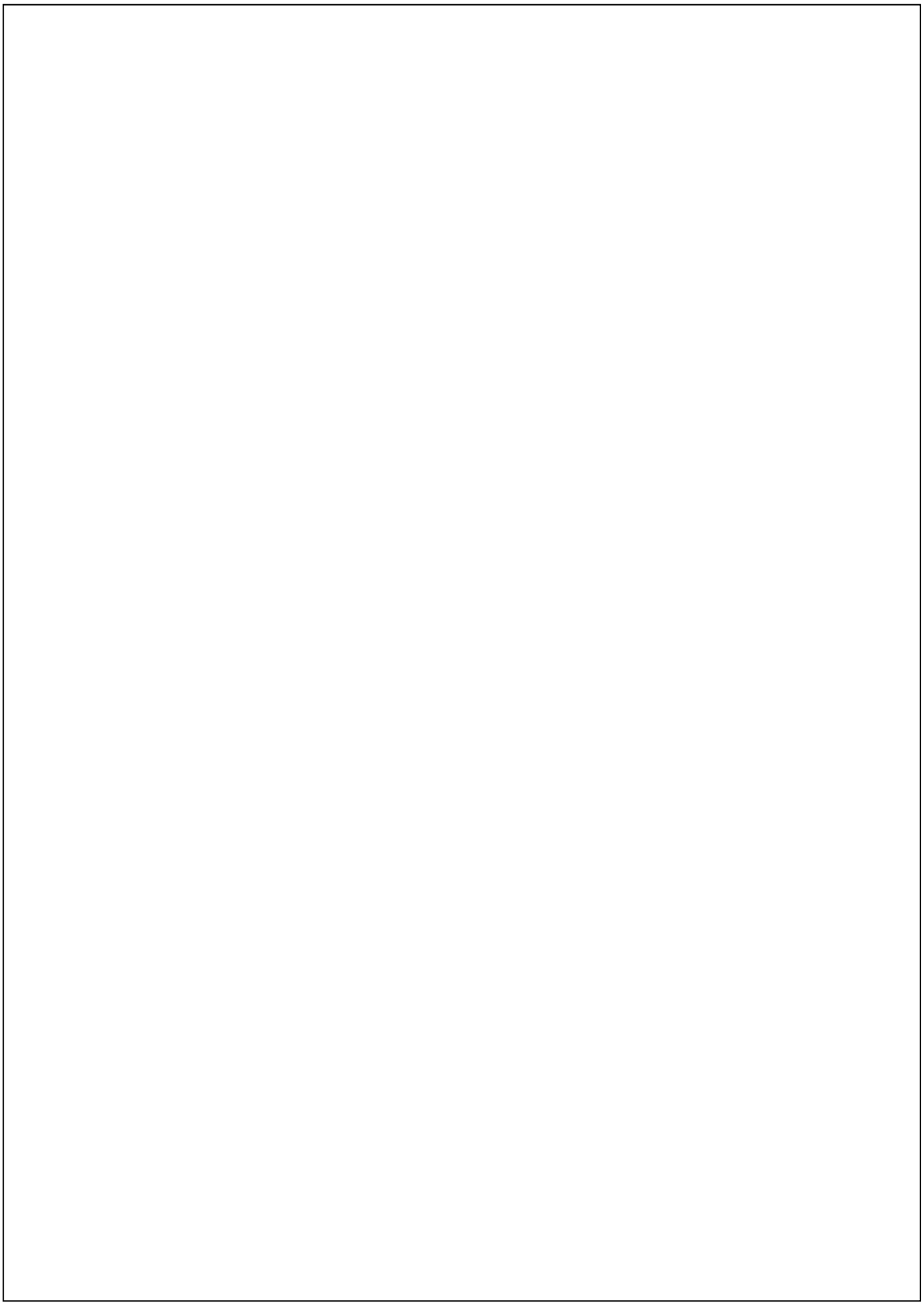

ace-21334.pdf

ORIGINALITY REPORT

8%	%	8%	%
SIMILARITY INDEX	INTERNET SOURCES	PUBLICATIONS	STUDENT PAPERS

PRIMARY SOURCES

1	Eray Baran, Mustafa Mahamid, Mehmet Baran, Metin Kurtoglu, Ines Torra-Bilal. "Performance of a moment resisting beam-column connection for precast concrete construction", Engineering Structures, 2021 Publication	2%
2	Kusnadi, R Djamaluddin, B Muhiddin, R Irmawaty. "The bonding strength of GFRP bars embedded within concrete under direct pull-out test", IOP Conference Series: Earth and Environmental Science, 2020 Publication	1%
3	B.B. Deshmukh, S.B. Jaju. "Design and Analysis of Glass Fiber Reinforced Polymer (GFRP) Leaf Spring", 2011 Fourth International Conference on Emerging Trends in Engineering & Technology, 2011 Publication	1%
4	Liu, Ruifen, and Chris P. Pantelides. "Shear strength of GFRP reinforced precast	1%

lightweight concrete panels", Construction and Building Materials, 2013.
Publication

---

5 Zhiqi Li, Yipeng Liu, Liangliang Qi, Zhonghao Mei, Ruize Gao, Muhuo Yu, Zeyu Sun, Ming Wang. "Optimization of the Laminate Structure of a Composite Cylinder Based on the Combination of Response Surface Methodology (RSM) and Finite Element Analysis (FEA)", Molecules, 2022 — 1%
Publication

---

6 Xu, P.. "Finite element analysis of burst pressure of composite hydrogen storage vessels", Materials and Design, 200908 — 1%
Publication

---

7 Liu, P.F.. "Recent developments on damage modeling and finite element analysis for composite laminates: A review", Materials and Design, 201009 — <1%
Publication

---

8 E Alizadeh, M Dehestani, B Navayi Neya, Mahdi Nematzadeh. "Efficient composite bridge deck consisting of GFRP, steel, and concrete", Journal of Sandwich Structures & Materials, 2017 — <1%
Publication

---

9 Lam, L.. "Design-oriented stress-strain model for FRP-confined concrete", Construction and — <1%

Building Materials, 200309/10
Publication

10 Lifeng Wang, Haiqi Wu, Long Liu, Ziwang Xiao. "Enhancement of local concrete compression performance byincorporating ultra-high performance concrete (UHPC) tube", Multidiscipline Modeling in Materials and Structures, 2022 <1 %
Publication

11 "Experimental Thermodynamics Volume II", Springer Science and Business Media LLC, 1968 <1 %
Publication

12 A Amir, R Djamaluddin, R Irmawati, A A Amiruddin. "Effect steel reinforcement ratio on the behavior of RC beam without concrete at tension zone using truss-system reinforcement", IOP Conference Series: Earth and Environmental Science, 2020 <1 %
Publication

13 Karam Mahmoud, Ehab El-Salakawy. "Effect of Transverse Reinforcement Ratio on the Shear Strength of GFRP-RC Continuous Beams", Journal of Composites for Construction, 2016 <1 %
Publication

14 T. Hilmansyah, H. Parung, R. Djamaluddin. "Pengaruh Ikatan Diagonal GFRP Pada Hubungan Balok Kolom Pracetak Terhadap <1 %

Kekuatan Sambungan", REKONSTRUKSI TADULAKO: Civil Engineering Journal on Research and Development, 2021
Publication

Exclude quotes	On	Exclude matches	< 4 words
Exclude bibliography	On		